BMC Infectious Diseases

RESEARCH

Open Access

Bayesian spatiotemporal modelling and mapping of malaria risk among children under five years of age in Ghana

Wisdom Kwami Takramah[1,2*†], Yaw Asare Afrane[2,3] and Justice Moses K. Aheto[2,4,5,6†]

Abstract

Background Malaria is a significant public health problem, particularly among children aged 6–59 months who bear the greatest burden of the disease. Malaria transmission is high and more pronounced in poor tropical and subtropical areas of the world. Climate change is positively correlated with the geographical distribution of malaria vectors. There is substantial evidence of spatial and temporal differences in under-five malaria risk. Thus, the study aimed to create intelligent maps of smooth relative risk of malaria in children under-5 years in Ghana that highlight high and low malaria burden in space and time to support malaria prevention, control, and elimination efforts.

Method The study extracted and merged data on malaria among children aged 6–59 months from the 2014 Ghana Demographic and Health Surveys (GDHS), 2016 and 2019 Ghana Malaria Indicator Surveys (GMIS). The outcome variable of interest was the count of children aged 6–59 months with a positive test on the rapid diagnostic test (RDT) result. Bayesian Hierarchical spatiotemporal models were specified to estimate and map spatiotemporal variations in the relative risk of malaria. The existence of local clustering was assessed using the local indicator of spatial association (LISA), and the points were mapped to display significant local clusters, hotpot, and cold spot communities.

Results The number of positive malaria cases in children aged 6–59 months decreased marginally from 946.7 (36.4%) in 2014 to 603.6 (22.9) in 2019 DHS survey periods. Smooth relative risk of malaria among children aged 6–59 months has consistently increased in the Northern and Eastern regions between 2014 and 2019. Socioeconomic and climatic factors such as household size [Posterior Mean: -0.198 (95% CrI: 3.52, 80.95)], rural area [Posterior Mean: 1.739 (95% CrI: 0.581, 2.867)], rainfall [Posterior Mean: 0.003 (95% CrI: 0.001, 0.005)], and maximum temperature [Posterior Mean: -1.069 (95% CrI: -2.135, -0.009)] were all shown as statistically significant predictors of malaria risk in children aged 6–59 months. Hot spot DHS clusters (enumeration areas) with a significantly high relative risk of malaria among children aged 6–59 months were repeatedly detected in the Ashanti region between 2014 and 2019.

Conclusion The findings of the study would provide policymakers with practical and insightful information for the equitable distribution of scarce health resources targeted at reducing the burden of malaria and its associated mortality among children under five years.

Keywords Malaria, Bayesian hierarchical model, Spatiotemporal modeling, Ghana, Children under-five years

†Wisdom Kwami Takramah and Justice Moses K. Aheto contributed equally to this work.

*Correspondence:
Wisdom Kwami Takramah
takramah@uhas.edu.gh
Full list of author information is available at the end of the article

Background

Malaria is a significant public health issue, particularly among children aged 6–59 months who bear the greatest burden of the disease. Malaria is among the top leading causes of mortality and morbidity in developing countries and increasingly becoming a major public health problem worldwide. Malaria transmission is high and more pronounced in underdeveloped tropical and subtropical areas of the world. The burden of malaria is tremendously pronounced in Southeast Asia, the Western Pacific, Latin America, and sub-Saharan Africa [1]. Malaria transmission is heterogeneous such that; even in endemic countries, those living in rural areas are at the greatest risk.

Malaria transmission is not observed in all parts of malaria-endemic countries [2]. Thus, this explains the spatial structure of malaria transmission. There is strong evidence of an association between malaria transmission and the geographical distribution of *Anopheles dirus* in the South-East Asia Region, Western Pacific Region [1] and other parts of the world. The malaria vectors such as *Anopheles gambiae* sensu lato, *Anopheles rufipes*, *Anopheles funestus* sensu lato, *Anopheles coluzzii* and *Anopheles stephensi* are found in Ghana and other countries in West Africa [3, 4]. Furthermore, climate change is positively correlated with the geographical distribution of malaria vectors. Thus, there is substantial geographical and temporal differences in under-five malaria risk.

Weather conditions such aridity, aridity rainfall, temperature, a high frequency of *Plasmodium falciparum*, an efficient vector, socio-demographic factors and insufficient malaria control and prevention methods are all strongly linked to malaria transmission in Africa. A deeper understanding of malaria transmission requires statistical modeling of socio-demographic factors, the environment, malaria vectors, and parasites that interact in a complex relationship to predict the risk and spatial distribution of malaria. Over the years, a variety of mathematical models have been developed to aid in understanding the malaria transmission mechanism, improving control strategies, and reducing the global impact of malaria. The very first malaria model was developed by Ronald Ross in 1911 [5, 6].

In 2018, children under the age of five years were the most vulnerable category, accounting for 67% of all malaria deaths worldwide. Sub-Saharan Africa has the largest malaria burden, accounting for more than 90% of all malaria deaths, with 78% of these deaths ascribed to children under the age of five years [7]. The current study centered on spatiotemporal modeling of the risk of malaria in children between the ages of 6 and 59 months, who account for most malaria cases in Sub-Saharan Africa region. This population experiences the highest burden of malaria, making it crucial to understand and predict the dynamics of the disease in this age group. It is vital to note that malaria and under-five mortality are threats to achieving Sustainable Development Goals (SDG) 3.2 which indicates that all countries should reduce neonatal deaths to 12 deaths per 1000 live births and under five deaths to 25 deaths per 1000 live births by 2030 [7].

Ghana is a malaria-endemic country with notable seasonal variations in the northern and southern ecological zone of the country. There was a rise in confirmed malaria cases from 3.6 million cases in 2014 to 5.5 million in 2018 in Ghana [8]. In Ghana, malaria is responsible for about 20,000 deaths in children annually, of which 25% are those aged < 5 years. Malaria prevalence in children aged 6 to 59 months is 8.6% according to microscopy results [9].

Over the years, Ghana has achieved tremendous progress in malaria prevention and control by establishing programs such as long-lasting insecticidal nets (LLINs), indoor residual spraying (IRS) of insecticides and malaria vaccines (RTS, S and R21) [3]. Nonetheless, malaria remains a public health problem in Ghana, accounting for a significant share of morbidity and mortality in the general population.

Spatiotemporal models have been used by scientists and mathematicians to estimate and map the spatiotemporal variation in the risk of malaria in children under five years over the years in Ghana and other parts of the world. Spatiotemporal modelling of routine health facility data for malaria risk micro-stratification in mainland Tanzania showed a marked spatial heterogeneity in malaria test positivity rate (TPR) across wards [10]. Another study on identifying malaria hotspots regions in Ghana using Bayesian spatial and spatiotemporal models revealed that numerous regions in Ghana are hotspots for malaria risk, yet climate and economic factors have no significant influence on malaria risk [11]. A previous study on spatiotemporal heterogeneity of malaria morbidity in Ghana demonstrated heterogeneity in the dynamics of malaria morbidity across the country [12]. To understand the spread and dynamics of malaria among children aged 6–59 months, the application of spatiotemporal modeling cannot be overemphasized. A spatiotemporal model of malaria among children aged 6–59 months is an analytical approach that combines geographical and temporal data to understand and predict the incidence and distribution of malaria cases in a specific population group. This type of model takes into account both the spatial variation, such as location or proximity to malaria risk factors, and the temporal variation, such as seasonal patterns or trends over time.

The prevention and control of malaria transmission require actionable spatial information for the equitable distribution of scarce health resources. Thus, the application of Bayesian Hierarchical spatiotemporal statistical model to estimate and map spatiotemporal variation in malaria in children aged 6–59 months is of utmost interest since the findings from this study will help inform policies to reduce malaria transmission in Ghana.

Materials and methods

Study population

The data on malaria cases among children aged 6–59 months was extracted from three secondary sources namely 2014 Ghana Demographic and Health Surveys (GDHS), 2016 and 2019 Ghana Malaria Indicator Surveys (GMIS) datasets using the biomarker questionnaire. The GDHS and GMIS are nationally representative cross-sectional household sample surveys. The sampling frame used for the 2014 GDHS, 2016 and 2019 GMIS was based on the 10 regional boundaries as defined according to the 2010 Population and Housing Census (PHC). The GDHS and GMIS used two stage sampling technique. In the first stage, enumeration areas were selected using probability proportional to size while in the second stage, households were selected using systematic sampling technique. The objective of the GMIS is to estimate malaria indicators for the 10 administrative regions, rural and urban areas [13].

The GDHS and GMIS used the Woman's Questionnaire to collect data on background characteristics, reproductive history for the last 5 years, preventive malaria treatment during the pregnancy of the most recent live birth, prevalence and treatment of fever among children under age 5 years, and exposure to and source of media messages about malaria in the last 6 months from women aged 15–49 years. The Biomarker Questionnaire was also used to collect data on the malaria and anaemia testing results of children aged 6–59 months. Rapid diagnostic test (RDT) and blood smears (expert microscopy) were used for malaria testing. This study used the results obtained from RDTs because they offer a useful, scalable, and effective diagnostic tool that makes them ideal for Ghana's healthcare system, particularly in poor and rural areas with limited access to lab facilities. The differences in diagnostic techniques, particularly between RDTs and microscopy, have an impact on the trends in malaria prevalence that have been reported. RDTs provide quick and easy diagnosis, but because antigens can be detected after therapy, they may overestimate the number of cases. However, because of technical difficulties, microscopy, despite being the gold standard, is prone to underreporting in areas with limited resources. Comparisons across regions and time periods may become more difficult as a result of these diagnostic disparities, which might produce artificial variations in prevalence trends. In the future, integrated data techniques and standardized diagnostic procedures will improve the dependability of malaria surveillance. In the 2014 GDHS, interviews were successfully conducted with 9,396 eligible women aged 15–49 years, including 4,716 from urban areas and 4,680 from rural areas. Similarly, the 2016 GMIS completed interviews with 5,150 eligible women aged 15–49 years, comprising 2,369 urban dwellers and 2,781 rural dwellers. In 2019, the GMIS interviewed 5,181 eligible women aged 15–49 years, drawn from households consisting of 2,440 urban and 2,741 rural dwellers. Access to the shapefiles used for the base layer of the maps was granted by DHS program upon request. The shapefiles used for the base layers of the maps were downloaded from the DHS program website upon registration and request [13]. Detailed information on terms of use of the shapefiles (GPS datasets) can be accessed at the DHS program website [14].

Outcome variable

The outcome variable of interest was the number of children aged 6–59 months with positive test result on rapid diagnostic test (RDT) in each sampled cluster aggregated at the regional and DHS cluster levels.

Independent variables

The covariates selected for this study were based on previous studies [9, 10] and are presented in Table 1. Through an examination of the theoretical underpinnings

Table 1 Independent variables

Variable	Type of variable
Outcome variable	
Malaria among children aged 6–59 months	Count
Explanatory variables	
Environmental factors	
Median aridity	Continuous
Median maximum temperature	Continuous
Median land surface temperature	Continuous
Median rainfall	Continuous
Median wet days	Continuous
Median itn coverage	Continuous
Median population density	Continuous
Group level factors	
Number of male children	Count
Number of female children	Count
Birth order	Count
Proportion of rural dwellers	Proportion
Median household size	Count

of the socioeconomic and environmental factors carefully selected from the literature, readers can gain a better understanding of the association between these factors and malaria risk. It will become more clearer why these variables were selected and how they affect the dynamics of malaria transmission if these links are highlighted. The environmental factors that were studied include median aridity (state of being extremely dry due to lack of rainfall), median maximum temperature (the highest temperature recorded during a specified period of time), median land surface temperature (the temperature of the Earth's surface, or how hot the ground would feel to the touch), median rainfall (amount of rain that falls in a place during a particular period), median wet days (a day that experiences precipitation), median insecticide-treated nets (ITNs) coverage and median population density. These environmental covariates were explored in a previous study [9]. The following individual-level and socio-economic factors were aggregated at the regional and DHS cluster level: number of male children, number of female children, proportion of rural dweller, median household size. These socioeconomic factors were explored in a previous study [10].

Statistical analysis

The study utilized data from both GDHS and GMIS surveys conducted in 2014, 2016 and 2019 which were imported into RStudio version 2023.09.1, Posit Public Benefit Corporation (PBC), Massachusetts, United States. Data extraction and analysis were done in 2023 and 2024. Trend analysis may be impacted by data inconsistencies because GDHS is conducted every five years and GMIS every two years. For example, using only GDHS data from more widely spaced-out years may change the appearance of trends seen in biannual GMIS data. Prevalence estimates and trend comparisons across space and time may be impacted by measurement biases introduced by variation in diagnostic techniques, especially with GMIS, and the use of self-reported symptoms for some GDHS data points. GMIS focuses on high-risk populations such as children under five and pregnant women which could introduce selection bias, potentially inflating malaria prevalence when generalized to the broader population. To eliminate detectable noise from the data, pre-processing and cleaning were carried out in Stata version 15 and RStudio version 2023.09.1. To produce clean data for analysis, duplicate checks and data consistency were carried out. We looked for potential mistakes in data input and collecting for the study variables. To make sure each category was exhaustive and mutually exclusive, the categorical variables were examined by ensuring that no data fell outside of the defined categories and there was no overlap between the categories. A box plot and histogram were also used to look for outliers in the quantitative variables.

The models included features of the survey design, including sample weights, stratification, and clustering. The DHS statistics guidance states that weighting is required for all DHS-generated data. This is because survey design features including unequal probability of sample selection, clustering, and stratification lead to data complexity. In order to account for variations in the likelihood of selection and interview between cases in a sample, adjustment factors such as sampling weights, clustering, and stratification were added to each case in tabulation.

The data were aggregated at the cluster level to investigate clustering of the relative risk of malaria among children aged 6–59 months. Given that the GDHS clusters display data at the point level, Stochastic Partial Differential Equation (SPDE) fitting of the Bayesian geospatial model was performed using the Integrated Nested Laplace Approximation (INLA) framework. The geographical and spatiotemporal areal count and point data were subjected to the INLA, which is a more computationally convenient and efficient parameter estimation method than other methods like Markov Chain Monte Carlo (MCMC) methods [15]. INLA approximates the posterior marginal distribution of the model parameters using a numerical integration approach for sparse matrices. Even though INLA is computationally efficient, it can introduce biases into the estimation, particularly in models with significantly skewed posterior distributions or highly non-linear models. INLA produces accurate marginal posteriors for most practical purposes; nonetheless, the approximation may not fully capture the complexity of the posterior for parameters with heavy-tailed or multimodal distributions. When modeling spatial dependency in spatiotemporal models, INLA usually uses predefined structures such as Gaussian Markov Random Fields (GMRFs). The model may produce less-than-ideal results if the spatial relationships in the data substantially depart from these presumptions. Global Moran's I statistics was employed to test spatial autocorrelation in the observations using a binary distance matrix. To achieve this, sets of neighbors were created based on their proximity. A spatial test for clustering was performed by assigning row standardized binary weights to the neighbor list, using minimum distance for one neighbor. Normality checks on the relative risk of malaria among children aged 6–59 months revealed a skewed distribution. Integrated Nested Laplace Approximation (INLA) framework was applied to the spatiotemporal areal count malaria data to estimate posterior distribution of the parameters of interest. Spatial structured random effects or correlated heterogeneity was assessed using

conditional autoregressive (CAR) model [16, 17] and temporal correlation was tested using random walk of order 1 (RW1) model. The besag CAR prior for the spatial component was specified. Based on the result of the autocorrelation test, Bayesian Hierarchical Spatiotemporal models were specified to smooth the data and identify spatiotemporal variations in the relative risk of malaria. Since environmental factors such as temperature, humidity, and rainfall have a significant impact on malaria transmission, the Bayesian hierarchical spatiotemporal model was applied to enable dynamic modeling of these time-varying factors and how they interact with patterns of malaria transmission. The Bayesian hierarchical spatiotemporal model that has been specified is most preferred because it is excellent at capturing temporal autocorrelation and spatial dependencies, both of which are critical for malaria research as environmental factors change over time and space (across regions and DHS clusters). In Ghana where malaria surveillance data may be incomplete or irregular, the specified Bayesian hierarchical spatiotemporal model is advantageous because it borrows strength from neighboring regions and adjacent time points to improve estimates for regions and DHS clusters or time periods with sparse data. This helps avoid biases that might arise from missing data, which can be more challenging to handle in other spatiotemporal models. The existence of local clustering was assessed using local indicator of spatial association (LISA) and the points were mapped to display significant local clusters, hotpot and cold spot areas [15]. A number of competing models including spatial and non-spatial Bayesian hierarchical models were specified to fit the lattice and geostatistical data. The Watanabe Akaike Information Criterion (WAIC) and the Deviance Information Criterion (DIC) were used to assess these models. The model that best fits the data has the lowest DIC and WAIC score. It is imperative to note that WAIC has several advantages over DIC since it closely approximates Bayesian cross-validation, it uses the entire posterior distribution, and it is invariant to parameterization [18, 19]. The WAIC and DIC are two commonly used metrics for model comparison, particularly in Bayesian modeling. Both criteria aim to balance model fit and complexity to select models that generalize well to new data, but they differ in their approach and assumptions.

To measure the degree of uncertainty surrounding the posterior mean of model parameter estimations, the 95% credible intervals were determined.

Model formulation

Standardized incidence ratio (SIR)/relative risk

The general spatiotemporal models for areal unit data when time is discrete were proposed and widely applied in diverse fields [15, 20, 21]. Let Y_{it} denote count of malaria among children aged 6–59 months in geographical region i and in time (i.e., year in our case) t, E_{it} represents expected count of malaria cases among children aged 6–59 months in geographical region i and year t, n_{it} refers to the number of persons at risk at geographical region i in year t.

The expected count of malaria among children aged 6–59 months in geographical region i in year t is defined as:

$$E_{it} = n_{it}\frac{\sum_{it} Y_{it}}{\sum_{it} n_{it}} \tag{1}$$

The formula for estimating relative risk (θ_{it}) of malaria among children aged 6–59 months in each geographical region i at year t is:

$$\widehat{\theta}_{it} = \frac{Y_{it}}{E_{it}} \tag{2}$$

The focus of the modeling is to estimate the log relative risk;

$$\mathbf{log}(\boldsymbol{\theta_{it}}) = \boldsymbol{\psi_{it}}$$

where θ_{it} denotes relative risk and ψ_{it} denotes log relative risk.

Bayesian hierarchical spatiotemporal poisson model

To model the smooth relative risk of malaria among children aged 6–59 months, we assumed malaria count Y_{it} observed in region i in year t follows a Poisson distribution and the model defined as a three-level process Bayesian Hierarchical model (BHM):

Data model:

$$Y_{it}|\psi_{it} \sim Poisson(E_{it}e^{\psi_{it}}), \tag{3}$$

Process model: [22–24]

$$\psi_{it} = \alpha + X_{it}\prime\boldsymbol{\beta} + \mu_i + \upsilon_i + \gamma_t + \varnothing_t \tag{4}$$

Parameter model:

$$\alpha \sim N(0, \tau_0^{-1})$$

$$\boldsymbol{\beta} \sim N(0, \tau_{\boldsymbol{\beta}}^{-1})$$

$$\upsilon_i \overset{iid}{\sim} N(0, \tau_{\upsilon}^{-1})$$

$$\mu_i|\mu_{j\neq i} \sim N(\overline{\mu}_i, \frac{1}{\tau_{\mu} m_i}),$$

$$\gamma_t \Big| \gamma_{t-1} \sim N(\gamma_{t-1}, \tau_\gamma^{-1})$$

$$\varnothing_t \sim N(0, \tau_\varnothing^{-1})$$

$$\text{now } \tau_0 \overset{iid}{\sim} logGamma(1, 0.001), \tau_\beta \overset{iid}{\sim} logGamma(1, 0.001)$$

$$\tau_V \overset{iid}{\sim} logGamma(1, 0.00005) \text{ and } \tau_\mu \overset{iid}{\sim} logGamma(1, 0.00005)$$

$$\tau_\gamma \overset{iid}{\sim} logGamma(1, 001) \text{and } \tau_\varnothing \overset{iid}{\sim} logGamma(1, 0.00005),$$

Where, Y_{it} is count of malaria among children aged 6–59 months in geographical region i at year t, E_{it} represents the standardized expected count in geographical region i at year t and ψ_i denotes the log relative risk in geographical region i in year t, α denotes the intercept term, $X_{it}\prime$ is a vector of predictors, $\boldsymbol{\beta}$ represents vector of regression parameters, μ_i represents spatial structured random effect which were assigned CAR model, υ_i represents unstructured spatial random effect among the locations at year t which is independently and identically distributed and γ_t represents correlated temporal random effects which were assigned a random walk-in time of first order ($\gamma = 1$). $\varnothing_t$ represents uncorrelated random effect which is independently and identically distributed and $\overline{\mu}_i$ is the mean of the neighboring μ_j values, m_i denote the number of neighbors of region i, $\frac{1}{\tau_\mu m_i}$ denote the variance for region i, τ_μ denotes precision parameter which controls the degree of smoothness or extra-Poisson variability assigned to clustering μ_i, τ_v denotes a precision parameter that controls the magnitude of the υ_i. All parameters such as α, β, μ_i, υ_i, τ_v, τ_μ are assigned prior distributions in the Bayesian modelling paradigm.

The uninformative priors on the log of the precision of the hyper-parameters included $\tau_0 \sim logGamma(1, 0.001)$ for intercept, $\tau_\beta \sim logGamma(1, 0.001)$ for fixed effects. $\tau_\mu \sim$ logGamma (1, 0.00005) for structured spatial random effect and $\tau_v \sim logGamma(1{,}0.00005)$ for unstructured spatial random effect [16, 20, 25–27]. The prior on the precision of unstructured temporal effect included $\tau_\varnothing \sim logGamma(1, 0005)$ and the prior specification of $\tau_\gamma \sim logGamma(1{,}0.001)$ on the precision of random walk of first order (RW1) was used [28]. The Bayesian model employed in this study incorporates parameters for population trend, using uninformative priors and hyperpriors based on prior research and expert input. Key assumptions include conditional independence of observations and Gaussian error terms, aligning with the objectives of identifying spatial dependencies. This model was selected based on the fact that a similar model was specified in a previous study [11]. Nonetheless, two Bayesian spatiotemporal models with and without covariates were specified and evaluated using WAIC and DIC, and the model that best fit the data was selected.

Geostatistical modelling of point referenced data

The study also applied a pure Bayesian Hierarchical Geospatial model to examine the relative risk and geospatial clustering of children aged 6–59 months with positive test on rapid diagnostic test (RDT) result.

Let Y_i denotes the number of children aged 6–59 months with positive test on rapid diagnostic test (RDT) kit out of a total of N_i children drawn from each of the geographical regions. We assume that Y_i out of N_i follows a binomial distribution presented as:

$$Y_i | P(s_i) \sim Binomial(N_i, P(s_i)), \tag{5}$$

$$\text{logit } (P(s_i)) = \beta_0 + d(\mathrm{x_i})'\beta + Z(s_i) \tag{6}$$

where β_0 is the intercept parameter which is assigned Gaussian prior with mean and precision to be zero (0), *d(.)* is a vector of observed environmental and climatic covariates, β is a vector of spatial regression coefficients for the covariates assigned Gaussian prior with mean zero (0) and precision 0.001, and Z(.) is a spatially structured random effect which follows a zero-mean Gaussian process with variance σ^2 and a given correlation function.

$$\rho(\mu) = corr\{Z(s_i), Z(s_j)\} \tag{7}$$

where u is the Euclidean distance between locations s_i and s_j and there are various parametric families for ρ(μ) [29]. The current study used the Matérn class of covariance function [30] given by

$$Cov\ (Z(s_i),\ Z(s_j)) = \frac{\sigma^2}{2^{\upsilon-1}\Gamma(\upsilon)}(\kappa \parallel s_i \parallel)^{\upsilon}\kappa_\upsilon(\kappa \parallel s_i - s_j \parallel) \tag{8}$$

where σ^2 denotes the variance of the spatial field, $\boldsymbol{\upsilon}$ is the shape parameter which determines the smoothness of *Z(s)*, so that Z(s) is $\nu - 1$ times mean-square differentiable and the scale parameter $\kappa > 0$ is related to the practical range $p = \frac{\sqrt{8\upsilon}}{\kappa}$ which is the distance at which the spatial correlation is negligible, and $K_\upsilon(.)$ is the modified Bessel function of second kind and order $\upsilon > 0$.

The spatial model was implemented under the Stochastic Partial Differential Equations (SPDE) approach using the integrated nested Laplace approximation (INLA) [31]. The study generated mesh for inference and prediction to support the SPDE strategy because the geostatistical data points in this study do not have explicit neighbours required by the SPDE strategy. Thus, the point referenced

Table 2 Demographic characteristics

	2014 GDHS			2016 GMIS			2019 GMIS		
	Total	**Negative n(%)**	**Positive n(%)**	**Total**	**Negative n(%)**	**Positive n(%)**	**Total**	**Negative n(%)**	**Positive n(%)**
Sex of child									
Male	1371	870.2 (63.5)	500.5 (36.5)	2977	2115(71.0)	862.1(29.0)	1330	1008(75.8)	321.7(24.2)
Female	1228	781.8 (63.7)	446.2 (36.3)	2823	2072(73.4)	751.2(26.6)	1303	1021(78.4)	281.9(21.6)
Age of child (in months)									
<12	265.5	215.3 (81.1)	50.18(18.9)	628.5	506.2(80.5)	122.3(19.5)	282	252.7(89.6)	29.34(10.4)
23–24	586.8	387.2 (66.0)	199.6 (34.0)	1313	1008(76.8)	304.5(23.2)	575.7	461.8(80.2)	113.9(19.8)
24–35	581.6	377.4 (64.9)	204.2(35.1)	1355	970.8(71.6)	384.7(28.4)	614.9	474.4(77.2)	140.5(22.8)
36–47	576.5	330.7 (57.4)	245.8(42.6)	1186	806.6(68.0)	379.7(32.0)	578.6	433.1(74.8)	145.6(25.2)
48–59	588.2	341.3 (58.0)	246.9 (42.0)	1317	895(68.0)	422.1(32.0)	581.1	406.7(70.0)	174.3(30.0)
Birth order									
1	527.7	384.9 (72.9)	142.8 (27.1)	1149	897.7(78.1)	251.2(21.9)	510.2	406(79.6)	104.2(20.4)
2	451.5	324 (71.8)	127.5 (28.2)	1086	837.6(77.1)	248.2(22.9)	542.3	428.6(79.0)	113.7(21.0)
3	384.4	254.9 (66.3)	129.5 (33.7)	878.7	648.9(73.9)	229.8(26.2)	376.8	311.8(82.7)	65.04(17.3)
4	339.4	193.8 (57.1)	145.6 (42.9)	673.9	492.8(73.1)	181.2(26.9)	320.8	243.2(75.8)	77.57(24.2)
5+	564.2	286.3 (50.8)	277.9(49.2)	1237	723.7(58.5)	512.8(41.5)	496.6	354(71.3)	142.6(28.7)
Birth interval									
<24 months	207.8	99.4(47.8)	108.4(52.2)	384.5	252.8(65.7)	131.7(34.3)	*187.2*	148.4(79.3)	38.75(20.7)
24–47 months	846.3	473.7(56.0)	372.6(44.0)	1124	805.7(71.7)	318(28.3)	470.8	358.7(76.2)	112.1(23.8)
48+ months	678.6	479.4(70.6)	199.2(29.4)	89.58	72.38(80.8)	17.2(19.2)	40.63	31.64(77.9)	8.991(22.1)
Has mosquito net for sleeping									
No	621.7	428.6 (69.0)	193(31.0)	912.9	681.1(74.6)	231.9(25.4)	372.8	306(82.1)	66.78(17.9)
Yes	2399	1449(60.4)	950(39.6)	4887	3506(71.7)	1381(28.3)	2259	1723(76.2)	536.8(23.8)
Type of residence									
Urban	1379	1126(81.7)	252.9(18.3)	2585	2253(87.2)	331.3(12.8)	1067	964(90.3)	103.3(9.7)
Rural	1641	750.8(45.8)	890.1(54.2)	3215	1933(60.1)	1282(39.9)	1565	1065(68.0)	500.4(32.0)
Household size									
8+ members	507.8	217.1(42.8)	290.7(57.2)	1115	673.8(60.4)	441(40.6)	651.1	461.7(70.9)	189.4(29.1)
5–7 members	1434	882.3(61.5)	551.6(38.5)	2683	1927(71.8)	756.5(28.2)	1158	915.7(79.0)	242.7(21.0)
1–4 members	1078	777.8(72.1)	300.7(27.9)	2002	1586(79.2)	415.8(20.8)	822.9	651.3(79.2)	171.5(20.8)
Household wealth index									
Poorest	694.1	262.2(37.8)	431.9(62.2)	1298	629.6(48.5)	668.2(51.5)	633.2	410.2(64.8)	223(35.2)
Poorer	644.8	268.5(41.6)	376.3(58.4)	1199	691.8(57.7)	507(42.3)	580.6	386.4(66.6)	194.1(33.4)
Middle	611	387.6(63.4)	223.5(36.6)	1172	879.4(75.1)	292.1(24.9)	553.3	430.4(77.8)	122.9(22.2)
Richer	561.7	488.4(87.0)	73.28 (13.0)	1183	1060(89.6)	123.4(10.4)	475.5	424.4(89.3)	51.06(10.7)
Richest	508.6	470.6(92.5)	38.09(7.5)	949	926.4(97.6)	22.66(2.4)	389.8	377.3(96.8)	12.45(3.2)

data do not have neighbourhood structure to define correlation between neighbours, so the mesh was produced to provide information about the spatial structure.

Results

Table 2 shows that the proportion of male (36.5%) and female (36.3%) children aged 6–59 months who tested positive for malaria using RDT in 2014 is the same. However, data from 2016 and 2019 revealed that a male child was more likely than a female child to contract malaria. In 2014, a child aged 48–59 months had the highest proportion of malaria cases (42.0%), followed by a child aged 23–24 months (34.0%). In 2016 and 2019, there was a positive association between the proportion of malaria cases and the age of the child.

Furthermore, data from 2014, 2016, and 2019 showed that a child with birth order 1 has a lower proportion of malaria than a child with birth order 2, that a child with birth order 2 has a lower proportion of malaria than a child with birth order 3, that a child with birth order

3 2 has a lower proportion of malaria than a child with birth order 4, and so on. In 2014, 2016, and 2019, it was discovered that a child with a birth interval of less than 24 months is more susceptible to malaria than a child with a birth interval of 24–47 months or 48 months and above.

Malaria in children aged 6–59 months who sleep under a mosquito net decreased during the three survey years (2014, 2016 and 2019). Despite the fact that malaria in children aged 6–59 months is more prevalent in rural regions than in urban areas across the three-year period, this has decreased with time. According to the findings from 2014, 2016, and 2019, a child in a family with 8 or more people is more likely to develop malaria than a child in a household with fewer than 8 members. Finally, in 2014, 2016, and 2019, a child from a low-income household is more likely to contract malaria.

Regional distribution of observed malaria prevalence

The observed prevalence of malaria by region according to rapid diagnostic test (RDT) results for the survey years are presented in Fig. 1. Notably, the prevalence rates of malaria in children aged 6–59 months across the regions steadily decreased over the survey years (2014–2019). There is substantial evidence of regional and temporal variations in the prevalence of malaria in children aged 6–59 months in Ghana.

Table 3 shows the global spatial autocorrelation coefficients calculated for each GDHS and GMIS survey year using aggregated GDHS and GMIS cluster level data. Under the null hypothesis of spatial randomness, the p-values obtained for Global Moran's I tests suggested the presence of strong spatial clustering but slightly weak autocorrelation. Because of the presence of clustering, the Bayesian Hierarchical geospatial and Spatiotemporal model were specified to smooth the malaria data. As a result, maps were created to demonstrate the spatial clustering of malaria in children aged 6–59 months.

Variable selection

Covariates were aggregated at both the regional and GDHS cluster levels. The Akaike Information Criterion (AIC) score favored 9 candidate covariates in the current study (median household size, median altitude, median wet days, number of rural dwellers, median rainfall, median ITN coverage, median maximum temperature, median aridity median, land surface temperature). Furthermore, a multicollinearity test was ran with a threshold of 10 to determine the presence of collinearity between the covariates. As a result, covariates having a variance inflation factor (VIF) value larger than 10 were eliminated from the models. Even though the VIF scores for median maximum temperature and land surface temperature exceeded the threshold of 10, we included them in the model because according to literature temperature contributes to malaria transmission (Table 4).

Model selection and validation

Table 5 displays the validation of competing models such as the Bayesian Hierarchical Spatiotemporal model without covariates (model 1) and with covariates (model 2), utilizing model validation methods such as DIC and WAIC. Based on the DIC or WAIC score, the best model was picked. A smallest DIC or WAIC score suggests that the model's prediction quality is better. As a result, model 2 had a lower DIC and WAIC score of 294.44 and 320.58, respectively. Therefore, Model 2 was selected as the most suitable for fitting the Bayesian hierarchical spatiotemporal framework. Lower values generally indicate a better-fitting model, and consistent values across models suggest good convergence.

Table 6 displays the results of the evaluation of the Poisson and Binomial likelihood models using DIC, WAIC, and log-Likelihood. The Poisson likelihood model produced better predictive accuracy than the Binomial likelihood model, which had the lowest DIC (294.45) and WAIC (320.6) scores; therefore, the Poisson likelihood model was selected as the most appropriate model to fit the data.

Spatial and temporal correlation test using CAR and RW1 models

A test of spatial dependence or spatial autocorrelation in malaria among children aged 6–59 months using a conditional autoregressive (CAR) model reveals the presence of spatial correlation with a 95% credible interval (CrI) associated with the posterior mean of the precision of structured spatial random effect τ_{μ}^{-1} [Posterior Mean: 22,052.07 (95% CrI: 1471.80, 86276.66)]. The posterior mean of τ_{υ}^{-1} [Posterior mean: 5.54 (95% CrI: 1.32, 14.92)] indicated that most of the variations in the risk of malaria among children aged 6–59 months were explained by the intercept term α and the covariates in model 2.

The estimated posterior mean of the precision of structured temporal random effect (RW1) τ_{γ}^{-1} shows some temporal dependence [Posterior Mean: 24.39 (95% CrI: 3.52, 80.95)]. Both spatial and temporal random effects are significant. The existence of spatial and temporal correlation between the observations justifies the application of Bayesian Hierarchical model which combines the three sub-models (data, process and parameter models) to form the hierarchical structure and borrows strength across space and time to approximate marginal posterior distribution of model parameters using bayes theorem.

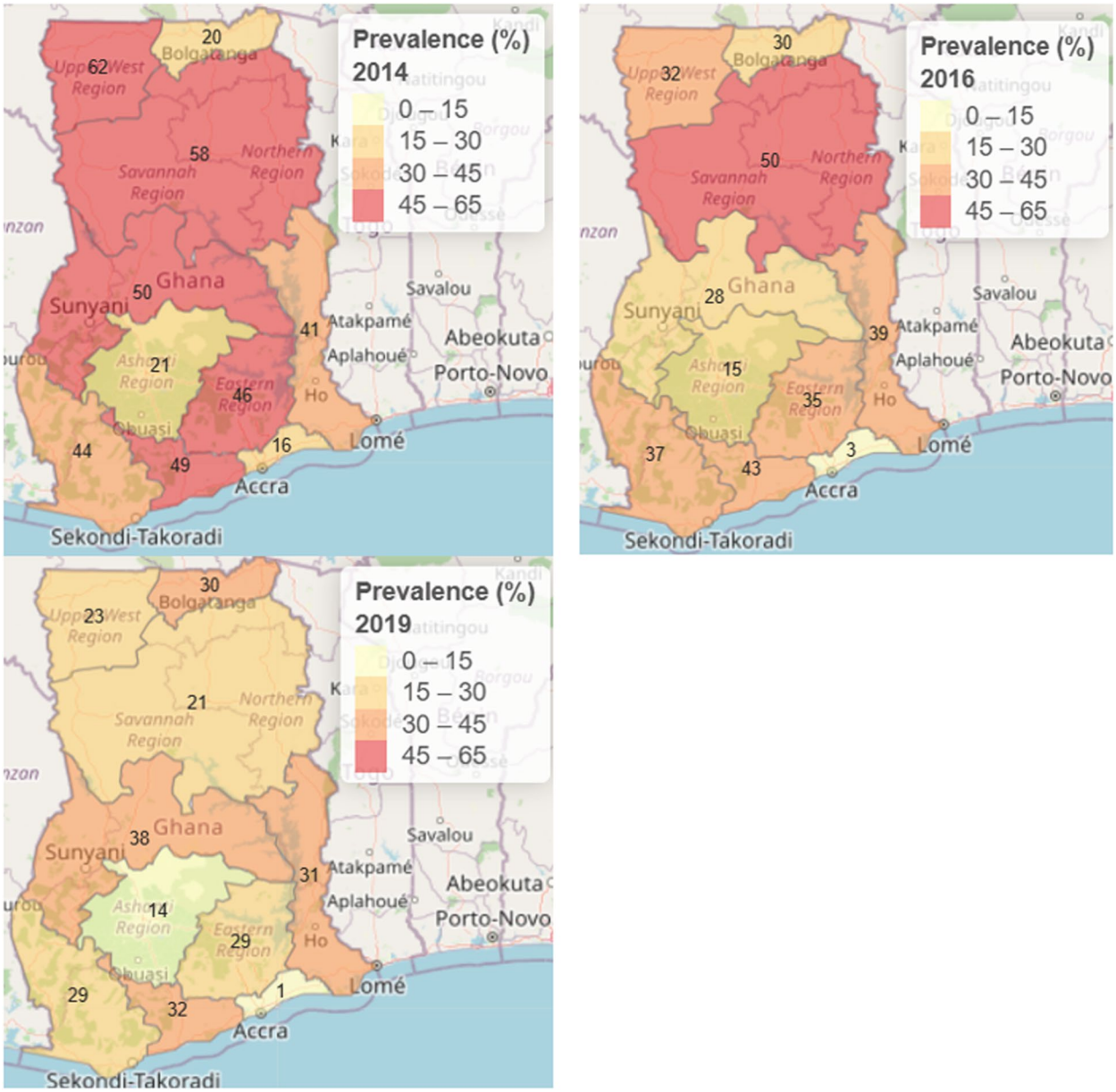

Fig. 1 Regional distribution of malaria prevalence (%) among children aged 6–59 months who tested positive for malaria by rapid diagnostic test (RDT) in 2014 (top left), 2016 (top right) and 2019 (bottom left). Note: The figures inserted in the maps are the percentage of children who tested positive for malaria. The same scale was used for the three survey years in the maps to allow for better comparison across the three survey years

Table 3 Estimating global spatial autocorrelation using Moran's I statistics for each survey year

Year	Moran's I statistics	*P*value
2014	0.214	< 0.0001
2016	0.269	< 0.0001
2019	0.220	< 0.0001

Distribution of model residuals

Figure 2 shows the presence of any spatial pattern in the distribution of the residuals across the DHS cluster level. The residuals are expressed in terms of standard deviations away from the mean. It is noticeable that 95% of the DHS clusters lie within −2 and 2 standard deviations. A spatial pattern of DHS clusters of under prediction, where the observed values are greater than the

Table 4 Multicollinearity test

Variables	Household size	Number of rural dwellers	Altitude	Median rainfall	ITN coverage	Median wet days	Median aridity median	Median maximum temperature	Land surface temperature	Threshold
VIF	2.195	3.808	1.695	4.138	2.843	5.389	6.449	12.234	14.232	10

Table 5 Evaluation of Bayesian Hierarchical Spatiotemporal model without covariates (model 1) and Bayesian Hierarchical Spatiotemporal model with covariates (model 2)

	DIC	WAIC
Model 1	327.24	367.49
Model 2	294.44	320.58

Model 1 = Bayesian Hierarchical Spatiotemporal model without covariates (empty model), Model 2 = Bayesian Hierarchical Spatioemporal model with covariates, *DIC* Deviance Information Criterion, *WAIC* Watanabe– Akaike information criterion

Table 6 Comparing poisson and binomial likelihood models for the dependent variable

Outcome variable	DIC	WAIC	log-Likelihood
Poisson	294.45	320.6	−228.5
Binomial	295.48	322.3	−229.16

predicted values (positive residuals) is observed. Spatial clusters of the residuals are not clearly noticeable.

Smooth relative risk of malaria among children aged 6–59 months across the then 10 regions in Ghana obtained from weighted Bayesian Hierarchical Spatiotemporal model with covariates

Figure 2 shows an upward trend in the relative risk of malaria among children aged 6–59 months from 2014 to 2019 in the Northern region. The relative risk of malaria among children aged 6–59 months has increased between 2014 to 2016 in the Upper East, Brong Ahafo and Eastern regions. The volta region recorded a low relative risk of malaria among children aged 6–59 months in 2014 and 2016; however, in 2019, there was a modest increase in this risk. Our results indicate that the relative risk recorded in the Ashanti region rose between 2014 and 2016 but decreased in 2019. Notably, from 2014 to 2016, the relative risk of malaria among children aged 6–59 increased in the Central region, but it decreased in 2019. In the Western region, the relative risk decreased between 2016 and 2019. Over the course of the three time periods, the Upper West and Upper East regions showed low relative risk.

Covariates associated with the risk of malaria among children aged 6–59 months obtained from weighted Bayesian Hierarchical Spatiotemporal model

Table 7 shows the estimated posterior means of covariates associated with the risk of malaria among children aged 6–59 months obtained from Bayesian Hierarchical Spatiotemporal Model. Covariates such as household size, rural area, wet days, rainfall, maximum temperature have all been shown as statistically significant predictors of malaria risk in children aged 6–59 months. The results showed that a unit increase in household size was likely to reduce the malaria risk among children aged 6–59 months [Posterior Mean: −0.198 (95% CrI: −0.329, −0.067)]. Our results indicate that children aged 6–59 months who live in rural areas have a higher risk of malaria [Posterior Mean: 1.739 (95% Cr.I: 0.581, 2.867)]. Furthermore, an increase in rainfall increases the incidence of malaria in children aged 6–59 months [Posterior Mean: 0.003 (95% CrI: 0.001, 0.005)]. Notably, among children aged 6–59 months, a unit increase in temperature is more likely to reduce the incidence of malaria [Posterior Mean: −1.069 (95% CrI: −2.135, −0.009)].

Local indicator of spatial autocorrelation (LISA) cluster map of relative risk of malaria among childing aged 6–59 months across GDHS clusters in Ghana obtained from geostatistical model

Clusters of hot and cold spots are displayed in Fig. 3. During the three-year period under examination, it was noted that the Eastern, Upper West, and Upper East regions did not record a significantly high relative risk of malaria among children aged 6–59 months. In the Northern region, hot spot clusters with a relative risk of malaria for children aged 6–59 months were discovered in 2014 and 2016, but as of 2019, these have disappeared. From 2014 to 2019, the Ashanti region continuously observed clusters with a considerably high relative risk of malaria among children aged 6–59 months. In the Greater Accra region, hot spot clusters were seen in 2014, but they disappeared in 2016 and 2019. In 2014 and 2016, the relative risk of malaria among children aged 6–59 months was not significantly high in the Western, Brong Ahafo, or Volta regions; however, in 2019, the risk has increased.

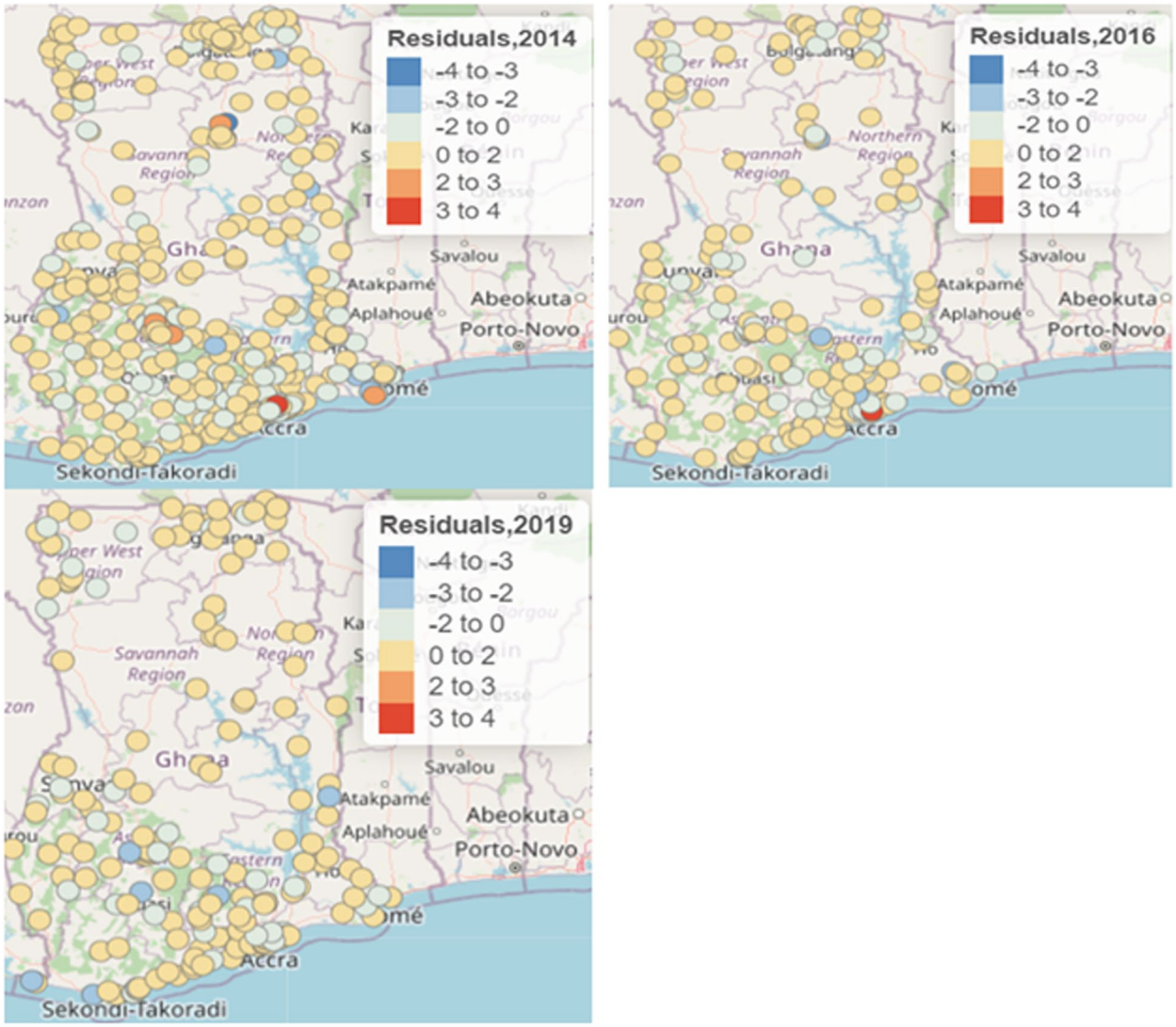

Fig. 2 Distribution of model residuals across DHS clusters

Discussion

The importance of reducing malaria among children under five years cannot be overemphasized. The findings of the current study which provide important insights into the current level of malaria control and elimination programs revealed that the number positive malaria cases decreased in children aged 6–59 months between the 2014 and 2019 DHS survey periods. Similar results of declining malaria cases among children under five years between 2014 and 2019 was reported in a previous study [7, 27]. The drop in malaria cases among children aged 6–59 months across the DHS survey years could be attributed to the government's successful and efficient malaria-elimination policies and programs, which were executed with help from development partners. Ghana has launched a nationwide Malaria Vaccine Implementation Programme (MVIP) in 2023, delivering RTS,S/AS01 malaria vaccines to children aged 6–59 months, with encouraging results as coverage of the first dose was 76% [32, 33]. Other malaria control and elimination interventions implemented by the government include residual spraying with overall spray coverage of 93.3% [34], long lasting treated net with coverage rate of 66.6% [35], Intermittent preventive treatment of malaria in pregnancy (IPTp) with coverage of 60% [35], and seasonal malaria chemotherapy (SMC) with amodiaquine–sulfadoxine-pyrimethamine (AQ-SP) with average cycle coverage of 93% [36] which are successfully protecting children under five years from malaria. The RTS,S malaria vaccine, indoor residual spraying (IRS), insecticide-treated

Table 7 Summary of posterior means and Bayesian credible intervals of smooth relative risk of malaria among children aged 6–59 months computed using aggregated Ghana demography and health survey (GDHS) and Ghana malaria indicator surveys (GMIS) regional level data from 2014 to 2019

	Model 1 Posterior mean (95 Cr.I)	Model 2 Posterior mean (95 Cr.I)
Fixed Effect		
Median Household size		−0.198(−0.329, −0.067)
Proportion of rural dwellers		1.739(0.581, 2.867)
Median altitude		0.001(−0.002, 0.003)
Median wet days		−0.164(−0.320, −0.009)
Median rainfall		0.003(0.001, 0.005)
Median ITN coverage		1.642(−0.982, 4.539)
Median temperature		−1.069(−2.135, −0.009)
median land surface temperature		0.232(−0.080, 0.556)
Median aridity		−0.030(−0.149, 0.091)
Random Effect		
	25,091.41(1936.97, 1.00e^05}	22,052.07 (1471.80, 86,276.66)
	2.94(1.31, 6.13)	5.54(1.32, 14.92)
	19.30(3.17, 58.9)	24.39(3.52, 80.95)
	26,196.78(2002.20, 1.06e^05)	21,954.68(1451.34, 86,028.50)
Model Evaluation Metrics		
DIC	327.24	294.44
WAIC	367.49	320.58

Model 1 = Bayesian Hierarchical Spatiotemporal model without covariates (empty model), Model 2 = Bayesian Hierarchical Spatiotemporal model with covariates, *DIC* Deviance Information Criterion, *WAIC* Watanabe– Akaike information criterion

nets (ITNs), and access to effective antimalarial medications are some of the malaria control measures that significantly influence the spatiotemporal trends in malaria burden that have been reported. Malaria prevalence and incidence vary geographically as a result of the effectiveness and coverage of malaria control measures, which are frequently region-specific. Over time, changes in the prevalence of malaria frequently correspond with the timing of intervention rollouts.

A global autocorrelation test using Moran's I Statistics under the null hypothesis of spatial randomness demonstrated spatial clustering in the observations at the DHS cluster level between 2014 and 2019 survey rounds. Thus, the presence of spatial clustering or autocorrelation justifies the use of Bayesian Hierarchical spatial modeling, which borrows strength across space to improve posterior approximation of marginal distribution of the model parameters [17]. Furthermore, Conditional Autoregressive (CAR) and Random Walk of order one (RW1) models were applied to the regional level aerial data, revealing the presence of spatial and temporal correlations, respectively, and justifying the use of Bayesian Hierarchical Spatiotemporal modeling to obtain smooth relative risk of malaria among children aged 6–59 months.

Model validation measures such as the Deviance Information Criterion (DIC) and the Watanabe- Akaike information criterion (WAIC) were used to validate Bayesian Hierarchical Spatiotemporal models with and without covariates. The Bayesian Hierarchical Spatiotemporal Model with covariates was chosen as the best performing model by both model validation measures. Additionally, we employed DIC and WAIC for model selection, leveraging their strengths in balancing model fit and complexity. DIC provided a straightforward measure for simpler hierarchical models, while WAIC accounted for predictive accuracy in more complex settings. Lower values of both criteria indicate better models, with WAIC being particularly robust for models with irregular posterior distributions. Thus, Bayesian Hierarchical Spatiotemporal model with covariates was specified to obtain smooth relative risk of malaria among children aged 6–59 months (Fig. 3).

The current study fitted Bayesian hierarchical spatiotemporal and geostatistical models to estimate and map patterns of malaria transmission among children aged 6–59 months in Ghana, using data from nationally representative surveys conducted in 2014 (GDHS), 2016 (GMIS), and 2019(GMIS). The findings of the current study show spatiotemporal variation in the relative risk

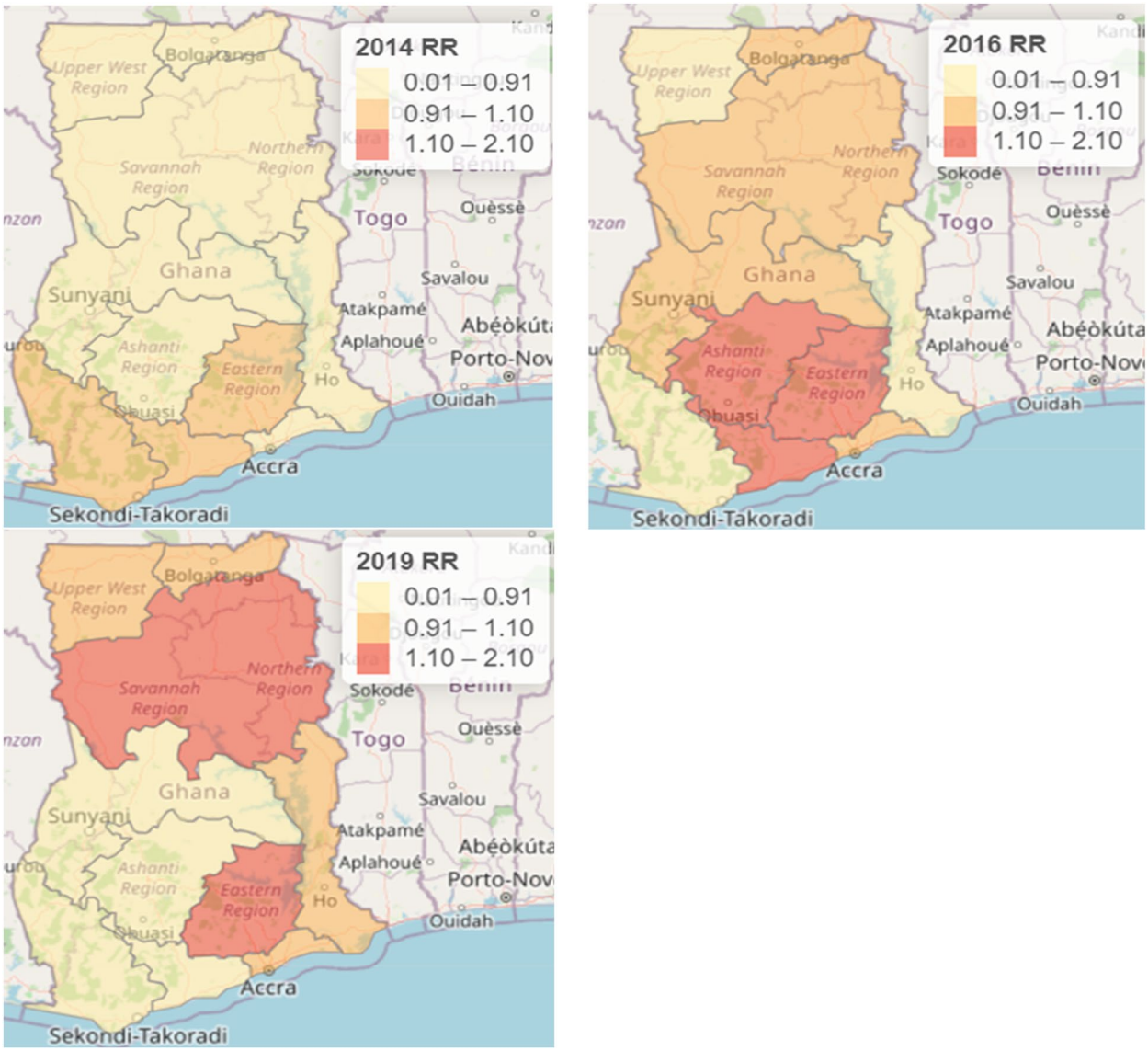

Fig. 3 Smooth relative risk of malaria among children aged 6–59 months according to RDT obtained from weighted Bayesian Hierarchical Spatiotemporal model with covariate

of malaria among children aged 6–59 months between 2014 and 2019. The findings showed that the relative risk of malaria varied across regions and time periods, with some regions exhibiting higher or lower risk than others, and some regions showing increasing or decreasing trends over time.

It is observed that malaria among children aged 6–59 months has consistently increased in the Northern and Eastern regions over the years. This finding was consistent with the results of a previous study carried out in Ghana [31]. The possible causes of the observed increase in malaria among children aged 6–59 months in the Northern and Eastern region include inadequate public health facilities, insufficient healthcare providers, illiteracy, and, most importantly poverty [3, 13, 37]. Despite the mountain of problems in the regions, healthcare providers must make appropriate use of scarce health resources in order to significantly reduce the number of malaria cases and other health events. Furthermore, during the survey years, the Volta region had a low relative risk of malaria among children aged 6–59 months. Malaria elimination interventions like residual spraying, long-lasting treated nets, seasonal malaria chemotherapy (SMC), improved health infrastructure, and a persistent commitment to malaria control and elimination may have been fully implemented in the Volta region where

malaria rates were significantly lower over the years. It was reported in the 2019 GMIS report that stockouts of RDTs in the Volta region and other regions may contribute to reduced rates of malaria among children aged 6–59 months. The statement may not mean that the actual prevalence of malaria reduced, but rather that the reported cases of malaria decreased due to the inability to confirm cases using RDTs. Without RDTs, health workers might not diagnose and record malaria cases accurately, leading to an artificial reduction in reported malaria rates. As a result, it is critical to guarantee that all health facilities have rapid diagnostic tests (RDTs) [3, 37].

The contrasting malaria trends in Volta and Ashanti regions are influenced by a complex interplay of socioeconomic, environmental, and programmatic factors. In Volta, high reliance on public health interventions and favorable environmental conditions have contributed to sustained declines in malaria burden. Conversely, Ashanti faces challenges stemming from urbanization and environmental conditions conducive to transmission. Addressing these disparities require targeted strategies, such as urban-specific vector control measures and enhanced community-based interventions in Ashanti, coupled with sustained efforts in Volta to ensure long-term gains. The current study found that the relative risk of malaria among children aged 6–59 months-in the Upper East, Central and Brong Ahafo regions increased somewhat between 2014 and 2016. In contrast, the trend in the Brong Ahafo and Central regions fell in 2019 and was steady in the Upper East region. Improvements in early malaria case diagnosis, malaria control, and now elimination initiatives have all contributed to a low relative risk in the Brong Ahafo and Central areas in 2019. Conversely, fluctuation in incidence of malaria among children under five years was observed in a study conducted in Nsanje District in Malawi between 2015 and 2019 [38].

The Bayesian Hierarchical Spatiotemporal Model, which was specified to estimate risk factors and map the spatial pattern of relative risk of malaria among children aged 6–59 months, identified some covariates that were significantly associated with the risk of malaria, such as household size, rural residence, wet days, rainfall, and maximum temperature. These covariates reflect the climatic and socioeconomic factors that influence malaria transmission and prevention. However, the findings of the current study did not align with the findings of a previous study which identified altitude as a major driver of malaria transmission [39].

The findings of the current study revealed that increasing household size is more likely to reduce the relative risk of malaria among children aged 6–59 months [Posterior Mean: −0.198 (95% CrI: 3.52, 80.95)]. A plausible explanation for this finding is that larger household size may help to reduce malaria among children aged 6–59 months because they have access to improved housing and sanitation facilities. Furthermore, larger households are more likely to practice collective malaria control and prevention measures such as vector control including the use of indoor residual spraying, mosquito coils and insecticide-treated bed nets.

Although it was found that larger households are more likely to lower the relative risk of malaria in children aged 6–59 months, it is crucial to note that a complex interplay of variables influences malaria prediction. Additionally, it is not possible to draw the conclusion that household size directly lowers malaria in children aged 6–59 months because socioeconomic factors have the potential to either strengthen or weaken this association. The direct impact of household size on malaria can be analyzed using mediation or moderation methods within a structural equation modeling framework; however, this approach was not employed in the current study.

The malaria control and prevention interventions help to curb the transmission and spread of malaria [34, 37].

It has been revealed in the current study that rural areas have a higher risk of malaria among children aged 6–59 months [Posterior Mean: 1.739 (95% Cr.I: 0.581, 2.867)] (Table 7). Similar results were found in a recent study that used data from a cross-sectional nationally representative malaria indicator survey conducted in Togo in 2017 [40]. A similar study conducted in Ghana revealed that data collected from the 2016 Ghana demographic and health survey also reported the similar results [30]. Another study conducted in Ghana on the topic "A predictive model, and predictors of under-five child malaria prevalence in Ghana: How do LASSO, Ridge and Elastic net regression approaches compare?" identified rural areas as a significant predictor of malaria in children under five years [41]. Rural areas throughout Africa are insufficient of essential health and other socioeconomic facilities, making them vulnerable to health problems and poverty [2]. In general, environmental conditions in rural communities are poor, serving as a breeding ground for malaria vectors that are not adequately controlled. This explains why rural areas have a higher risk of malaria.

In the current study, climate factors such as rainfall [Posterior Mean: 0.003 (95% CrI: 0.001, 0.005)] and maximum temperature [Posterior Mean: −1.069 (95% CrI: −2.135, −0.009)] influence malaria transmission among children aged 6–59 months. Malaria transmission is positively correlated with rainfall, but a unit increase in temperature resulted in a decrease in malaria transmission among children aged 6–59 months (Table 7). The finding from a previous study showed that with increasing

average temperatures in Ghana and Nigeria, the incidence rate of malaria decreased significantly between 2012- 2014 and between 2000 −2003. On the other hand, increase in temperatures at lower altitudes, where malaria and mosquitoes are already common, affect the growth cycle of the parasite that makes the mosquito carry the disease, enabling it to develop malaria more quickly and, consequently, increasing the rates of transmission [42, 43].

Climate change has been identified to have significant influence on malaria transmission in literature [42–44].

Climate change, such as increases in rainfall, humidity, and temperature, are more likely to multiply the mosquito population at higher altitudes, according to available data. As a result of the disease's wider geographical distribution caused by climate change, malaria tends to spread fast to new geographical places with no documented history of malaria endemicity [43]. Previous studies have found that higher rainfall was associated with an increase in the number of malaria cases [45] and rainfall intensity of 40–55 mm was more likely to cause malaria transmission [46]. Climate change is progressively becoming a major public health problem, attracting the attention of world leaders. As a result, world leaders and governments must accelerate measures to increase environmental and ozone layer education, as well as commit resources holistically to addressing climatic factors that cause malaria transmission and other climate change that endangers human life and existence.

Local indicator of spatial autocorrelation (LISA) cluster map of relative malaria risk among children aged 6–59 months across GDHS clusters in Ghana indicated hot and cold spot DHS clusters (Fig. 4). From 2014 to 2019, DHS clusters with a significantly high relative risk of malaria among children aged 6–59 months were repeatedly detected in the Ashanti region.

Despite the fact that the government of Ghana, through the Ministry of Health (MoH) and the Ghana Health Service, has instituted malaria control and prevention measures over the years to reduce malaria transmission and spread in the general population, malaria remains a significant public health problem. These measures have focused particularly on vulnerable groups such as children under the age of five, pregnant women, and the elderly. However, malaria continues to pose a significant challenge in the Ashanti region during the survey period under study.

Hot spot DHS clusters of significantly high relative risk of malaria among children aged 6–59 months was observed in the Greater Accra region in 2014, but disappeared in 2016 and 2019. This demonstrates the good work of the malaria control/elimination program and the regional health directorate in the Greater Accra region in reducing the threat of malaria among children aged 6–59 months. Conversely, regions such as Western, Brong Ahafo, or Volta regions were doing so well in malaria management in 2014 and 2016, however, hot spot of DHS clusters of malaria among children aged 6–59 months were observed in 2019.

Conclusion

In conclusion, there are spatial and temporal variations in the observed count of malaria among children aged 6–59 months across the regions and the survey periods. Thus, the current study evaluated and applied Bayesian Hierarchical spatiotemporal model that borrows strength across space and time to estimate and map spatiotemporal variation of malaria among children aged 6–59 months. The Bayesian Hierarchical spatiotemporal model with covariates was selected as the best performing model for estimating posterior mean of the model parameters based on the results of the model evaluation measures such as DIC and WAIC.

One of the key findings of the current study showed that the smooth relative risk of malaria among children aged 6–59 months obtained from Bayesian Hierarchical spatiotemporal model with covariates varied across regions and time periods, with some regions exhibiting higher or lower risk than others, and some regions showing increasing or decreasing trends over time. For instance, the relative risk of malaria among children aged 6–59 months in the Northern region has increased consistently from 2014 to 2019. Over the course of the survey years under consideration, the Upper West and Upper East regions showed low relative risk. Hot spot analysis using local indicator of spatial autocorrelation (LISA) consistently identified some DHS clusters as hot spot areas in the Ashanti region between 2014 and 2019 survey years. Another significant finding of the current study is that DHS clusters in regions such as the Eastern, Upper West, and Upper East regions did not record a significantly high or low relative risk of malaria among children aged 6–59 months. These regions can serve as a test case where regions with hot spot DHS clusters can learn from. Thus, further research should be carried out in these low-risk (cold-spots) malaria regions and lessons learnt should be transferred to the regions with hot spot DHS clusters.

Lastly, the Bayesian Hierarchical Spatiotemporal Model identified some covariates that were significantly associated with the risk of malaria, such as household size, rural residence, wet days, rainfall, and maximum temperature. These covariates reflect the climatic and socioeconomic factors that influence malaria transmission.

In conclusion, fitting a spatiotemporal model to estimate and map spatiotemporal variation in malaria among

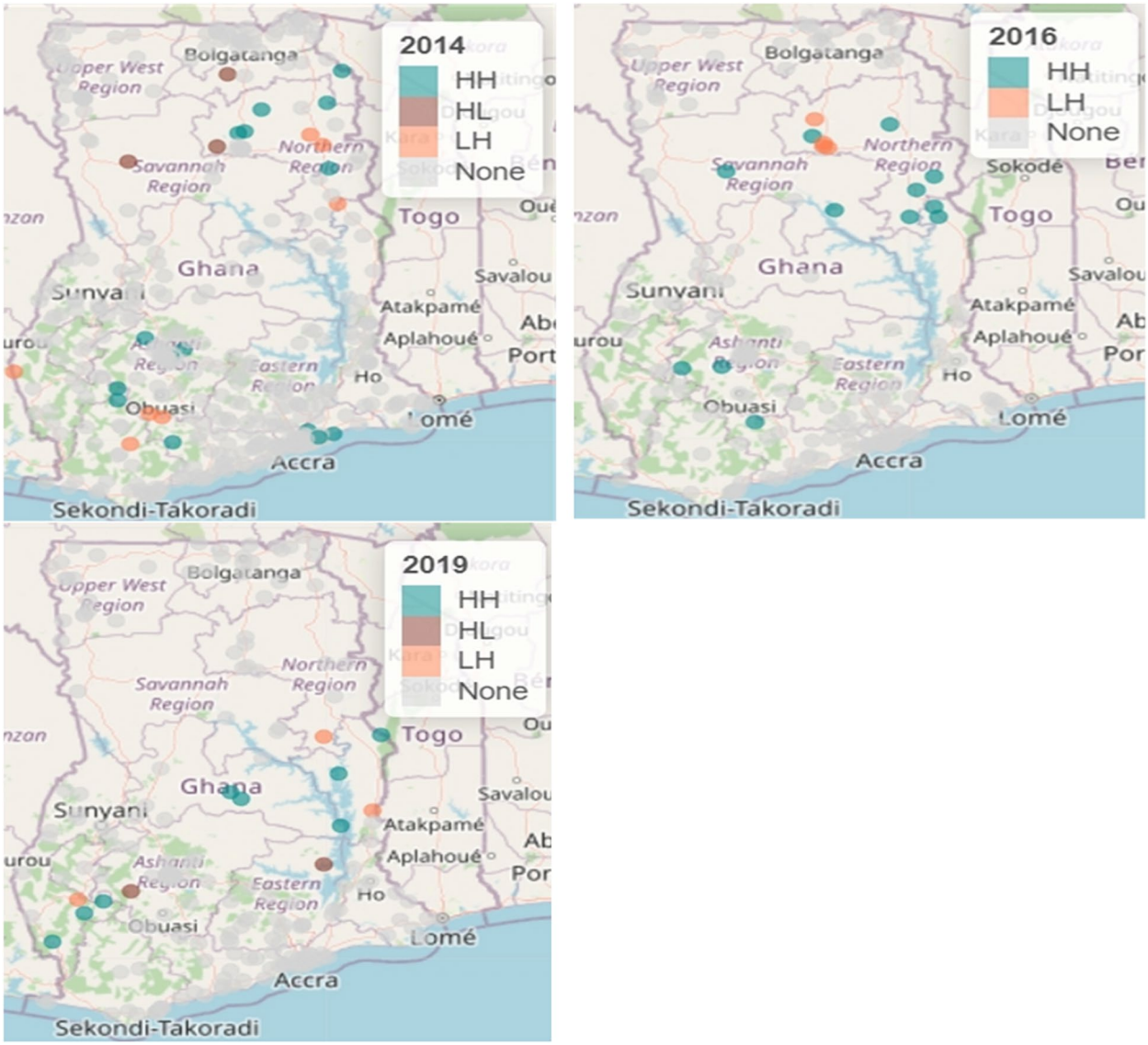

Fig. 4 LISA cluster map showing statistically significant relative risk of malaria among children aged 6–59 months according to RDT across GDHS clusters in Ghana obtained from geostatistical model, 2014–2019

children under the age of five in Ghana is a complicated and advanced geostatistical modeling method that must be carefully considered. The findings of the current study would provide policymakers with practical and insightful information for the equitable distribution of scarce health resources in order to fight and reduce the threat of malaria among children under five years. The findings can be used to develop pilot studies that evaluate how well focused interventions such as Insecticide-treated nets (ITNs) and Indoor residual spraying (IRS) work to lower the prevalence of malaria in high-risk areas, gradually improving control strategies. When allocating health resources, areas with persistently high transmission rates or recent spikes in malaria prevalence can be given priority expanding the number of medical personnel and diagnostic centers in regions where access to malaria testing and treatment is restricted. The findings can provide actionable information in deploying mobile health units in underprivileged regions that the model indicated in order to increase access to malaria testing and treatment. By concentrating on regions where interventions are most likely to have a major impact, policymakers can more effectively distribute funds, reduce waste, and increase cost-effectiveness. In regions where malaria is

highly prevalent, the results can help support large-scale implementation of proven interventions like mass drug administration (MDA).

Future research

Future research should focus on developing a predictive model that uses machine learning algorithms to forecast malaria in children under five years old given pertinent covariates including climate, socioeconomic status, urbanization levels, and individual and community-level determinant.

Limitation of the study

The acknowledged inconsistencies between GDHS and GMIS surveys, such as differences in sampling methods and measurement tools, may introduce biases in the data. These differences could affect the comparability of results, leading to potential measurement errors or limitations in generalizability. Despite these limitations, the overlapping objectives and robust methodologies of the two surveys support their integration for addressing the objectives of the study. Furthermore, self-reporting may be prone to social desirables and respondents may have recollection bias. Another limitation of the GDHS and GMIS data is the lack of monthly temporal resolution because these surveys are conducted every five years, which constrains the ability to analyze malaria seasonal trends in alignment with environmental factors such as climate variations. Additionally, the cross-sectional nature of the surveys limits the ability to assess seasonality or short-term fluctuations in malaria transmission and to assess causal relationships. The current study did not employ mediation or moderation methods within structural equation modeling framework to analyze the direct effects of the covariates on malaria in children aged 6–59 months.

Abbreviations

AIC	Akaike Information Criterion
AQ-SP	Amodiaquine–sulfadoxine-pyrimethamine
BHM	Bayesian Hierarchical model
CAR	Conditional Autoregressive
DIC	Deviance Information Criterion
GDHS	Ghana demography and health survey
HH	High-High
HL	High-Low
GMIS	Ghana malaria indicator surveys
INLA	Integrated nested Laplace approximation
IRS	Indoor residual spraying
LISA	Local indicator of spatial autocorrelation
LLINs	Long-lasting insecticidal nets
LH	Low–High
LL	Low–High
MoH	Ministry of Health
MVIP	Malaria Vaccine Implementation Programme
NMCP	Ghana National Malaria Control Programme
RDTs	Rapid diagnostic tests
RW1	Random Walk of order one
SMC	Seasonal malaria chemotherapy
SPDE	Stochastic Partial Differential Equations
VIF	Variance inflation factor
WAIC	Watanabe- Akaike information criterion

Acknowledgements

Special thanks go to DHS program for providing access to the datasets used in the current study. Dr. Wisdom Kwami Takramah is a WAMCAD Postdoctoral Fellow under the supervision of Prof. Justice Moses K. Aheto. Prof. Justice Moses K. Aheto is a British Council –Study UK Alumni Awardee.

Authors' contributions

W.K.T., J.M.K.A., and Y.A.A. participated in the conception of the study. W.K.T. and J.M.K.A. participated in the study design. W.K.T. and J.M.K.A. participated in data collection. W.K.T. and J.M.K.A. participated in the data analysis. W.K.T. and J.M.K.A. engaged in the interpretation of the results. W.K.T. and J.M.K.A. wrote the main manuscript. W.K.T., J.M.K.A., and Y.A.A. contributed to the writing and reviewing of the various sections of the manuscript. All authors read and approved the final manuscript.

Funding

This study was funded by a grant from the Bill and Melinda Gates Foundation (INV-047051) and the National Institute of Health (D43 TW 011513).

Data availability

The GDHS datasets are available on the Demographic and Health Surveys (DHS) program website (https://dhsprogram.com/data/Registration-Rationale.cfm) and can be accessed at no cost. However, registration is required for access to the data files.

Declarations

Ethics approval and consent to participate

The 2014 GDHS, 2016 and 2019 GMIS protocols were reviewed and approved by the Ghana Health Service Ethical Review Committee and the Institutional Review Board of ICF International. Thus, ethical permission for the current study was not needed since the required GDHS dataset was available publicly. However, ethical procedures were strictly observed at the time of the GDHS and GMIS surveys to ensure that human rights were protected as required by US Department of Health and Human Services. Detail information on DHS data and ethical standards can be accessed at: http://goo.gl/ny8T6X.

Consent for publication

Not applicable.

Competing interests

The authors declare no competing interests.

Author details

[1]Department of Epidemiology and Biostatistics, School of Public Health, University of Health and Allied Sciences, Ho, Ghana. [2]The West Africa Mathematical Modeling Capacity Development (WAMCAD) Consortium, Accra, Ghana. [3]Department of Medical Microbiology, University of Ghana Medical School, University of Ghana, Accra, Ghana. [4]Department of Biostatistics, School of Public Health, University of Ghana, Accra, Ghana. [5]WorldPop, School of Geography and Environmental Science, University of Southampton, Southampton SO17 1BJ, UK. [6]College of Public Health, University of South Florida, Tampa, FL, USA.

Received: 3 May 2024 Accepted: 11 March 2025
Published online: 28 March 2025

References

1. Santaguida PS, Raina P, Booker L, Patterson C, Baldassarre F, Cowan D, et al. Pharmacological Treatment of Dementia: Summary. AHRQ Evid Rep Summ. 2004;97(1998–2005):1–19. Available from: https://www.ncbi.nlm.nih.gov/books/NBK11963/.
2. CDC. Malaria's impact worldwide. Center for Disease Control and Prevention; 2020. Available from: https://www.cdc.gov/malaria/malaria_worldwide/impact.html.

3. Forson AO, Hinne IA, Dhikrullahi SB, Sraku IK, Mohammed AR, Attah SK, et al. The resting behavior of malaria vectors in different ecological zones of Ghana and its implications for vector control. Paras Vectors. 2022;15(1):1–14. https://doi.org/10.1186/s13071-022-05355-y.
4. Mnzava A, Monroe AC, Okumu F. Anopheles stephensi in Africa requires a more integrated response. Malar J. 2022;21(1):4–9. https://doi.org/10.1186/s12936-022-04197-4.
5. Ignacio M, Pablo J. Ross-Macdonald models : which one should we use ? Acta Trop. 2020;207. Available from: https://arxiv.org/pdf/2002.11267.pdf.
6. Ross R. Some a priori pathometric equations. Br Med J. 1915;1:546. Available from: https://www.bmj.com/content/1/2830/546.
7. UNCG, CSO. The sustainable development goals (SDGs) in Ghana. 2017. p. 1–40.
8. U.S. President's Malaria Initiative Ghana. Malaria operational plan FY 2020. 2020. Available from: https://d1u4sg1s9ptc4z.cloudfront.net/uploads/2021/03/fy-2020-ghana-malaria-operational-plan.pdf.
9. Aheto JMK. Mapping under-five child malaria risk that accounts for environmental and climatic factors to aid malaria preventive and control efforts in Ghana: Bayesian geospatial and interactive web-based mapping methods. Malar J. 2022;21(1):384.
10. Thawer SG, Golumbeanu M, Lazaro S, Chacky F, Munisi K, Aaron S, et al. Spatio-temporal modelling of routine health facility data for malaria risk micro-stratification in mainland Tanzania. Sci Rep. 2023;13(1):10600.
11. Iddrisu AK, Otoo D, Hinneh G, Kanyiri YD, Samuel KY, Kubio C, et al. Identifying malaria hotspots regions in Ghana using Bayesian spatial and spatiotemporal models. Infect Dis Immun. 2024;4(2):69–78.
12. Awine T, Malm K, Peprah NY, Silal SP. Spatio-temporal heterogeneity of malaria morbidity in Ghana: Analysis of routine health facility data. PLoS One. 2018;13(1):14.
13. Ghana Statistical Service, Ghana Health Service, ICF. Ghana malaria indicator survey (GMIS). 2017. p. 1–2.
14. Burgert CR. and Georeferenced Data Release Health Surveys Dhs Spatial Analysis Reports 7. 2013. Available from: https://dhsprogram.com/publications/publication-SAR7-Spatial-Analysis-Reports.cfm.
15. Otieno E, Okuto A. Bayesian spatial and spatiotemporal modelling. 2013.
16. Acharya B, Tabb L. Corrected : Spatiotemporal Analysis of Overall Health in the United States Between 2010 and 2018. Cureus. 13(9). Available from: https://pubmed.ncbi.nlm.nih.gov/3469235.
17. Morris M, Wheeler-martin K, Simpson D, Stephen J, Gelman A, Dimaggio C, et al. Bayesian hierarchical spatial models: implementing the Besag York Mollié model in Stan. 2018.
18. Cramb S, Baade P, Duncan E, Mengersen K. Investigation of Bayesian spatial models. 2017.
19. Vehtari A, Gelman A, Gabry J. Practical Bayesian model evaluation using leave-one-out cross-validation and WAIC. 2015. Available from: http://arxiv.org/abs/1507.04544.
20. Banerjee S, Carlin BP, Gelfand AE. Hierarchical modeling and analysis for spatial data. 2nd ed. Bunea F, Isham V, Keiding N, Louis T, Smith RL, HT, editor. New York: Taylor & Francis Group, LLC; 2015. p. 257.
21. Congdon P. Spatial heterogeneity in Bayesian disease mapping. GeoJournal. 2019;84(5):1303–16. https://doi.org/10.1007/s10708-018-9920-1.
22. Lindgren F, Rue H, Blangiardo M, Cameletti M, Baio G. Bayesian spatial and spatiotemporal modelling with R-INLA Spatial and Spatio-Temporal models with R-INLA . 2016. Available from: https://www.researchgate.net/publication/309760682.
23. Fah R', Rachmawati N, Djuraidah A, Fitrianto A, Made Sumertajaya I. Spatio-temporal models using R-INLA with generalized extreme value distribution in Hierarchical Bayes regression. 2018;4. Available from: www.ijsrset.com.
24. Moraga P. Geospatial health data: modeling and visualization with R-INLA and shiny. 2019;2019:1–2.
25. Aheto JMK, Utuama OA, Dagne GA. Geospatial analysis, web-based mapping and determinants of prostate cancer incidence in Georgia counties : evidence from the 2012 – 2016 SEER data. 2021. p. 1–13.
26. Aheto JMK, Menezes LJ, Takramah W, Cui L. Modelling spatiotemporal variation in under-five malaria risk in Ghana in 2016–2021. Malar J. 2024;23(1):102. Available from: https://malariajournal.biomedcentral.com/articles/10.1186/s12936-024-04918-x.
27. Jingyi Guo. R-INLA: An R -package for INLA. Department of Mathematical Sciences, NTNU. 2016. Available from: https://fuglstad.folk.ntnu.no/Lund2016/Session2/INLA_rinla.pdf.
28. Diggle PJ, Ribeiro P. Model-based geostatistics. New York: Springer; 2007.
29. Matern B. Spatial variation. Berlin: Springer-Verlag; 1986.
30. Miller DL, Glennie R, Seaton AE. Understanding the stochastic partial differential equation approach to smoothing. J Agric Biol Environ Stat. 2020;25(1):1–16. https://doi.org/10.1007/s13253-019-00377-z.
31. Yankson R, Anto EA, Chipeta MG. Geostatistical analysis and mapping of malaria risk in children under 5 using point - referenced prevalence data in Ghana. Malar J. 2019;18:1–12. https://doi.org/10.1186/s12936-019-2709-y.
32. Okyere J, Bediako VB, Ackah JA, Acheampong E, Owusu BA, Agbemavi W, et al. RTS, S/AS01E vaccine defaults in Ghana: a qualitative exploration of the perspectives of defaulters and frontline health service providers. Malar J. 2023;22(1):1–10. https://doi.org/10.1186/s12936-023-04690-4.
33. Asante KP, Mathanga DP, Milligan P, Akech S, Oduro A, Mwapasa V, et al. Feasibility, safety, and impact of the RTS, S/AS01E malaria vaccine when implemented through national immunisation programmes: evaluation of cluster-randomised introduction of the vaccine in Ghana, Kenya, and Malawi. Lancet. 2024;403(10437):1660–70.
34. USAID. Ghana end of spray report. Spray campaign: March 2–April 12, 2022. 2022.
35. Ghana Statistical Service (GSS) and ICF. Ghana Demographic and Health Survey 2022. 2022. Available from: https://dhsprogram.com/pubs/pdf/FR387/FR387.pdf.
36. Adjei MR, Kubio C, Buamah M, Sarfo A, Suuri T, Ibrahim S, et al. Effectiveness of seasonal malaria chemoprevention in reducing under-five malaria morbidity and mortality in the Savannah Region, Ghana. Ghana Med J. 2022;56(2):64–70.
37. Ghana National Malaria Control Programme (NMCP), Ghana Health Service (GHS), ICF. Ghana malaria indicator trends: 2014-2019. Accraand Rockville; 2021. Available from: https://dhsprogram.com/pubs/pdf/OD81/OD81.pdf. Cited 2023 Dec 16.
38. Gondwe T, Yang Y, Yosefe S, Kasanga M, Mulula G, Luwemba MP, et al. Epidemiological trends of malaria in five years and under children of nsanje district in Malawi, 2015–2019. Int J Environ Res Public Health. 2021;18(23):12784.
39. Dabaro D, Birhanu Z, Negash A, Hawaria D, Yewhalaw D. Effects of rainfall, temperature and topography on malaria incidence in elimination targeted district of Ethiopia. Malar J. 2021;20(1):104.
40. Kombate G, Gmakouba W, Scott S, Azianu KA, Ekouevi DK, van der Sande MAB. Regional heterogeneity of malaria prevalence and associated risk factors among children under five in Togo: evidence from a national malaria indicators survey. Malar J. 2022;21(1):168.
41. Aheto JMK. Predictive model and determinants of under-five child mortality : evidence from the 2014 Ghana demographic and health survey. 2019. p. 1–10.
42. Leal Filho W, May J, May M, Nagy GJ. Climate change and malaria: some recent trends of malaria incidence rates and average annual temperature in selected sub-Saharan African countries from 2000 to 2018. Malar J. 2023;22(1):248.
43. Moore S. The effect of climate change on malaria. 2022. Available from: https://www.news-medical.net/health/The-Effect-of-Climate-Change-on-Malaria.aspx. Cited 2023 Dec 22.
44. Ryan SJ, Lippi CA, Zermoglio F. Shifting transmission risk for malaria in Africa with climate change: a framework for planning and intervention. Malar J. 2020;19(1):170.
45. Tiu LA, Wahid WE, Andriani WY, Mirnawati, Tosepu R. Literature review: Impact of temperature and rainfall on incident Malaria. Bristol, England: IOP Conf Ser Earth Environ Sci. 2021;755(1).
46. Adeola A, Ncongwane K, Abiodun G, Makgoale T, Rautenbach H, Botai J, et al. Rainfall trends and malaria occurrences in Limpopo province, South Africa. Int J Environ Res Public Health. 2019;16(24):5156.

Publisher's Note